Anomalous thermodiffusion, absolute negative mobility, and reverse heat transport in a single quantum dot

Yanchao Zhang [*] and Xiaolong Lü
School of Science, Guangxi University of Science and Technology, Liuzhou 545006, People's Republic of China

(Received 16 August 2024; revised 4 January 2025; accepted 26 March 2025; published 9 April 2025)

We investigate the steady-state transport characteristics of a quantum dot system consisting of a single energy level embedded between two reservoirs under the influence of both the temperature gradient and bias voltage. Within tailored parameter regimes, the system can exhibit three counterintuitive transport phenomena of anomalous thermodiffusion, absolute negative mobility, and reverse heat transport respectively. These counterintuitive phenomena do not violate the second law of thermodynamics. Moreover, absolute negative mobility and reverse heat transport can be identified by a reversible energy level. These anomalous transports are different from thermoelectric transports and provide different perspectives for a more comprehensive understanding of the transport characteristics of quantum systems.

DOI: 10.1103/PhysRevE.111.044112

I. INTRODUCTION

In equilibrium thermodynamics, a temperature gradient can induce particle transport, even in the absence of a concentration gradient. Normally, the direction of the particle transport is the same as the direction of the temperature gradient, i.e., from high-temperature heat reservoir to low-temperature heat reservoir, this phenomenon is called thermodiffusion, also known as thermophoresis or Soret effect [1–4]. However, a somewhat counterintuitive phenomenon of particle flows moving against a temperature gradient known as anomalous thermodiffusion (AT) has also been found in different systems in recent years [5–7]. This counterintuitive transport phenomenon has stimulated new and extensive interest in exploring the novel transport behavior of thermodynamic systems.

When a system is in thermal equilibrium, the response of the system to an applied force is always in the same direction as the applied force, as it move toward a new equilibrium. Therefore, it is impossible for the system's response to be opposite to an applied force, which would violate the laws of thermodynamics. When the system deviates from thermal equilibrium under the action of the temperature gradient, the response of the system becomes possible in the opposite direction of the applied force. A typical example is the thermoelectric effect, where an applied force, i.e., the bias voltage, is applied to the system and acts in the opposite direction of the temperature gradient [8]. Based on the Seebeck effect, the particle current can move against the bias voltage driven by the temperature gradient, or based on the Paltier effect, the heat flow can flow from low-temperature heat reservoir to high-temperature heat reservoir against the temperature gradient driven by the bias voltage. The thermodynamic properties of these processes have been extensively studied in thermoelectric heat engines [9,10] and thermoelectric refrigerators [11,12].

However, when the applied force is in the same direction as the temperature gradient, an inverse response implies an induced current (e.g., either particle or heat) against both applied forces, which is highly counterintuitive, although there is no fundamental law that forbids abnormal phenomenon. In the study of particle transport, a counterintuitive behavior called absolute negative mobility (ANM) occurs, where the steady state particle current of the system is opposite to the thermodynamic force. In recent years, the ANM has been investigated in a variety of nonequilibrium systems, such as Brownian particles [13–22], microfluidic systems [23], Josephson junctions [24], two-dimensional incompressible laminar flow [25], one-dimensional interacting Hamiltonian system [26], Coulomb-coupled quantum dots system [27], active polymer [28], and active tracer particle [29,30]. Another counterintuitive behavior related to heat transport is known as reverse heat transport (RHT), where heat can flow from a low-temperature heat reservoir to a high-temperature heat reservoir against all thermodynamic forces. Recently, the RHT has also been found in both quantum [27,31,32] and classical systems [26].

In this paper, we focus on the steady-state transport characteristics of a single-level quantum dot system that deviates from the equilibrium when driven by temperature gradient and bias voltage. It can be found that in tailored parameter regimes, the system will exhibit counterintuitive transport phenomena, which are anomalous thermodiffusion, absolute negative mobility, and reverse heat transport, respectively. This paper is a further extension of the research based on Ref. [27]. However, the study in Ref. [27] has specificity, such as the presence of Coulomb interactions. This study begins with the most basic single-level quantum dot model and investigates the anomalous transport phenomena, generation conditions, and physical mechanisms of the system, offering a more fundamental and universal understanding. This paper

[*]Contact author: zhangyanchao@gxust.edu.cn

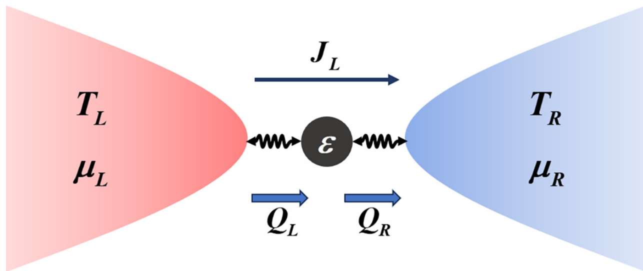

FIG. 1. The schematic diagram of a single quantum dot embedded between two reservoirs at different temperatures and chemical potentials.

is organized as follows. In Sec. II, the model and theory are detailed. In Sec. III, the AT phenomena is described. In Sec. IV, the ANM induced by thermal equilibrium fluctuation is analyzed. In Sec. V, the RHT is presented and the thermodynamic characteristics of the anomalous transport are analyzed. In Sec. VI, the thermoelectric transport is briefly discussed. In Sec. VII, the conclusions are summarized.

II. MODEL AND THEORY

We consider the simplest prototype model, which consists of a quantum dot with a single spinless energy level ε in contact with two reservoirs at different temperatures T_ν and chemical potentials μ_ν ($\nu = L, R$), as shown schematically in Fig. 1. In the limit of weak tunneling coupling, the broadening of energy level can be neglected, and the transmission through a tunnel barrier is well described by sequential tunneling of a single electron. The quantum dot can be occupied by at most one electron, and the system has only two quantum states, i.e., $|0\rangle$ and $|1\rangle$, with occupation probabilities described as p_0 and p_1. Thus, the time evolution of occupation probabilities is given by a master equation [9]

$$\frac{d}{dt}\begin{pmatrix} p_0 \\ p_1 \end{pmatrix} = \begin{pmatrix} -W_{10} & W_{01} \\ W_{10} & -W_{01} \end{pmatrix}\begin{pmatrix} p_0 \\ p_1 \end{pmatrix}, \tag{1}$$

where W_{10} and W_{01} are the transition rates from state $|0\rangle$ to state $|1\rangle$ and state $|1\rangle$ to state $|0\rangle$, respectively. The transition rates are given by Fermi's golden rule

$$W_{10} = \sum_{\nu=L,R} W_{10}^{\nu} = \sum_{\nu=L,R} \gamma_\nu f_\nu, \tag{2}$$

$$W_{01} = \sum_{\nu=L,R} W_{01}^{\nu} = \sum_{\nu=L,R} \gamma_\nu (1 - f_\nu), \tag{3}$$

where $f_\nu = [1 + e^{(\varepsilon-\mu_\nu)/k_B T_\nu}]^{-1}$ is the Fermi-Dirac distribution function, and γ_ν is bare tunneling rate. We are interested in the steady-state transport, which is given by the stationary solution of the Eq. (1), i.e., $dp_i/dt = 0$ ($i = 0, 1$) with $p_0 + p_1 = 1$, the occupation probabilities can be solved as

$$p_0 = \frac{W_{01}}{W_{01} + W_{10}}, \tag{4}$$

$$p_1 = \frac{W_{10}}{W_{01} + W_{10}}. \tag{5}$$

The steady-state current from the left reservoir to the quantum dot is then given by

$$J_L = W_{10}^{L} p_0 - W_{01}^{R} p_1 = \gamma (f_L - f_R), \tag{6}$$

where $\gamma = \gamma_L \gamma_R / (\gamma_L + \gamma_R)$, and $J_R = W_{01}^{R} p_1 - W_{10}^{L} p_0 = J_L$.

The steady-state heat flow from left reservoir and the steady-state heat flow into right reservoir are respectively given by

$$Q_L = (\varepsilon - \mu_L) J_L, \tag{7}$$

$$Q_R = (\varepsilon - \mu_R) J_R. \tag{8}$$

According to stochastic thermodynamics [9], the entropy production rate associated with the master equation is given by

$$s = \sum_{i,j,\nu} W_{ij}^{\nu} p_j \ln \frac{W_{ij}^{\nu} p_j}{W_{ji}^{\nu} p_i}. \tag{9}$$

This is consistent with the standard thermodynamic statement, i.e., $s = Q_R/T_R - Q_L/T_L$.

In our next numerical simulations, we set $T_L = T + \Delta T/2$ and $T_R = T - \Delta T/2$, where $T = (T_L + T_R)/2$ is the average temperature of the system, and $\Delta T = T_L - T_R$ is the temperature gradient. When $\Delta T > 0$, i.e., the left reservoir is at higher temperature, which is the forward configuration of the temperature gradient. $\mu_L = \mu + |e|\Delta V/2$ and $\mu_R = \mu - |e|\Delta V/2$, where $\Delta V = (\mu_L - \mu_R)/|e|$ is bias voltage, and $\Delta V > 0$ indicates the forward bias voltage. We set $\mu = 0$ as reference and use natural units, i.e., $k_B = |e| = \hbar = 1$.

III. ANOMALOUS THERMODIFFUSION

We first consider a simple case with $\Delta T > 0$ and $\Delta V = 0$, that is, the system only applies one positive temperature gradient. The curves of the steady-state current J_L and the steady-state heat flow Q_L with a single energy level ε at different system temperatures T are shown in Fig. 2. It can be found that the steady-state heat flow Q_L is always greater than zero, that is, the heat flows from the high-temperature reservoir to the low-temperature heat reservoir, which is the expected result. For the steady-state current J_L, when $\varepsilon > 0$, $J_L > 0$, i.e., the electrons will flow from the high-temperature reservoir to the low-temperature heat reservoirs. However, when $\varepsilon < 0$, the current of the electrons will reverse and flow from the low-temperature reservoir to the high-temperature heat reservoir. It is clear that thermodiffusion of electrons in single quantum dot system exhibits a counterintuitive phenomenon, where the electrons move against temperature gradient ΔT and accumulate in high-temperature heat reservoir. This phenomenon is called the anomalous thermodiffusion (AT). In Fig. 2, it can also be seen that as long as the single energy level $\varepsilon < 0$, the AT phenomena will appear regardless of the average temperature of the system.

According to Eq. (6), $J_L \propto \Delta f$, where $\Delta f = f_L - f_R$ represents the difference in electron distribution between the two heat reservoirs. When $\varepsilon > 0$, $\Delta f > 0$, this means that at the single level position, the electron distribution concentration of the left heat reservoir is greater than that of the right heat reservoir, which is equivalent to adding a driving force

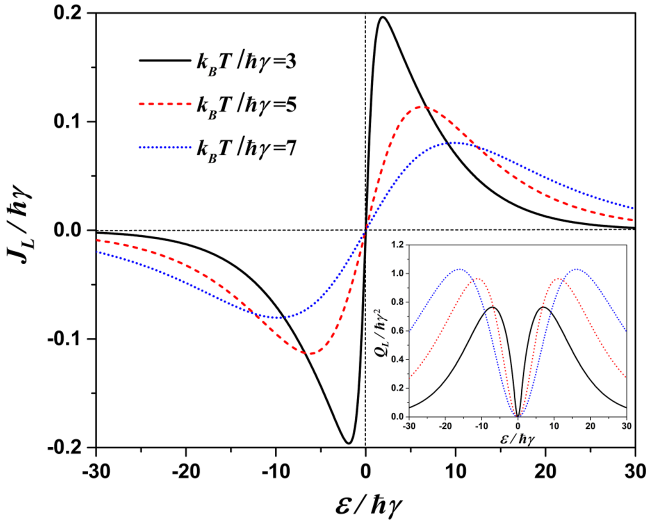

FIG. 2. The steady-state current J_L is depicted as a function of a single energy level ε at different system temperatures T. The anomalous thermodiffusion occurs when $\varepsilon < 0$. Inset: The steady-state heat flow Q_L as a function of a single energy level ε at different system temperatures T. The parameters $k_B\Delta T/\hbar\gamma = 5$, $|e|\Delta V/\hbar\gamma = 0$.

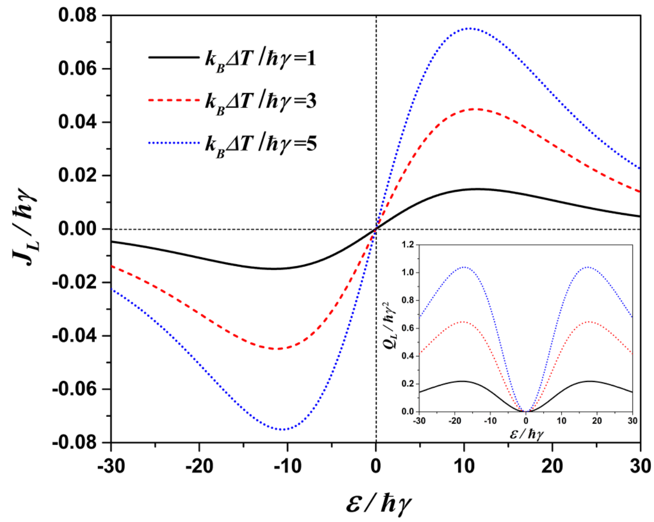

FIG. 3. The steady-state current J_L is depicted as a function of a single energy level ε at different temperature gradients ΔT. The anomalous thermodiffusion occurs when $\varepsilon < 0$. Inset: The steady-state current Q_L as a function of a single energy level ε at different temperature gradients ΔT. The parameters $k_BT/\hbar\gamma = 7.5$, $|e|\Delta V/\hbar\gamma = 0$.

(concentration gradient) in the direction of the temperature gradient causing the steady-state current to flow from the high-temperature heat reservoir to the low-temperature heat reservoir. However, when $\varepsilon < 0$, the electron concentration of the right heat reservoir at the energy level position is greater than that of the left heat reservoir. This is equivalent to applying a concentration gradient in the opposite direction of the temperature gradient, causing the steady-state current to exhibit AT behavior. Therefore, the AT is a transport process caused by the unbalanced concentration distribution of heat reservoirs on both sides of the energy level.

The steady-state current J_L and the steady-state current Q_L are depicted as a function of a single energy level ε at different temperature gradients ΔT, as shown in Fig. 3. It is found that as the temperature gradient ΔT increases, both the steady-state current J_L and the steady-state heat flow Q_L of the system are enhanced. This is due to the increase in temperature gradient, which intensifies the imbalance of electron concentration on both sides of the heat reservoir. Thus, the AT phenomenon of the system will become more significant.

IV. ABSOLUTE NEGATIVE MOBILITY

We now consider the transport characteristics of the steady-state current J_L in the presence of a forward bias voltage, i.e., $\Delta V > 0$. The steady-state current J_L is depicted in Fig. 4 as a function of a single energy level ε at different temperature gradients ΔT. It can be found that when the temperature gradient $\Delta T = 0$, that is, the system is in thermal equilibrium, the steady-state current J_L is always greater than zero, that is, it flows in the direction of bias voltage. When the system deviates from the thermal equilibrium state and a positive temperature gradient $\Delta T > 0$ is superimposed along the direction of the bias voltage, it is interesting that the steady-state current J_L of the system will be less than zero, that is, the steady-state current J_L flows backward against the bias voltage. This is because the temperature gradient induces AT when the system deviates from thermal equilibrium, as shown in Fig. 3. It can be observed that in the region where $\varepsilon < 0$, the AT induced solely by temperature gradient when $\Delta V = 0$ and $k_B\Delta T/\hbar\gamma = 5$ (blue dot line in Fig. 3), while in the same region, the forward current driven solely by bias voltage when $|e|\Delta V/\hbar\gamma = 5$ and $\Delta T = 0$ (black line in Fig. 4). When the system simultaneously applies temperature gradient and bias voltage, the forward current driven by the bias voltage will offset a portion of the AT induced by the temperature gradient, as shown in the blue dot line in Fig. 4. However,

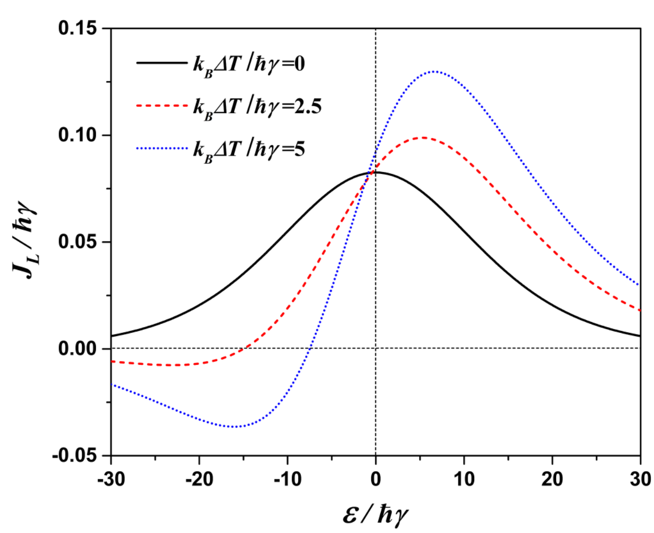

FIG. 4. The steady-state current J_L is depicted as a function of a single energy level ε at different temperature gradients ΔT. The absolute negative mobility occurs in regions where $\varepsilon < 0$ when $\Delta T > 0$. The parameters $k_BT/\hbar\gamma = 7.5$, $|e|\Delta V/\hbar\gamma = 5$.

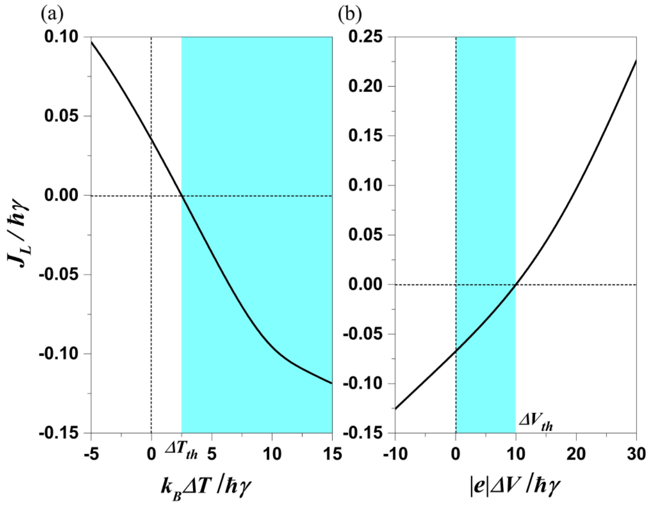

FIG. 5. The steady-state current J_L is depicted as a function of the temperature gradient ΔT for $|e|\Delta V/\hbar\gamma = 5$ (a) and as a function of the bias voltage ΔV for $k_B\Delta T/\hbar\gamma = 5$ (b), respectively. The absolute negative mobility occurs in blue region. The parameters $k_BT/\hbar\gamma = 7.5$, $\varepsilon/\hbar\gamma = -15$.

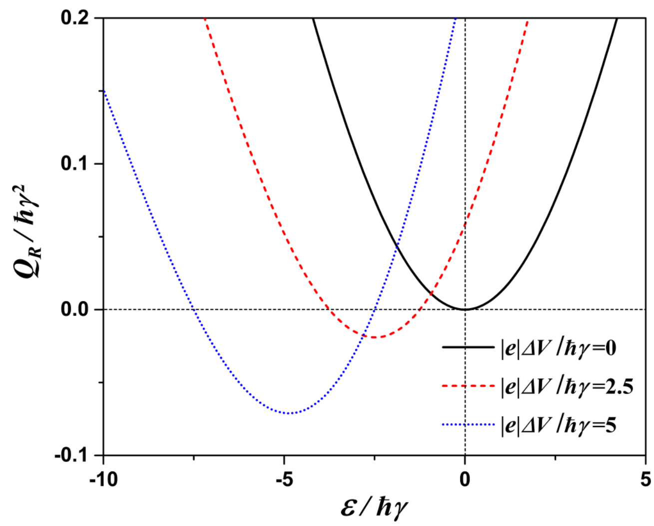

FIG. 6. The steady-state heat flow Q_R is depicted as a function of a single energy level ε at different bias voltages ΔV. The reverse heat transport occurs in regions where $\varepsilon < 0$ when $\Delta V > 0$. The parameters $k_BT/\hbar\gamma = 7.5$, $k_B\Delta T/\hbar\gamma = 5$.

there still exists the phenomenon of steady-state current less than zero, that is, transported against the bias voltage and the temperature gradient. This phenomenon is called absolute negative mobility (ANM). Obviously, the ANM is induced by thermal equilibrium fluctuation, and essentially, the ANM can be attributed to the AT that can be generated by temperature gradient overcoming bias voltage when the bias voltage is not large.

Figure 5 shows the steady-state current J_L as a function of the temperature gradient ΔT for $|e|\Delta V/\hbar\gamma = 5$ (a) and as a function of the bias voltage ΔV for $k_B\Delta T/\hbar\gamma = 5$ (b), respectively. It can be found in Fig. 5(a) that there is a threshold ΔT_{th} and $\Delta T_{th} = -T\Delta V/\varepsilon$ based on Eq. (6). In the range of $0 < \Delta T < \Delta T_{th}$, the steady-state current satisfies $J_L > 0$. This is because the forward current driven by the bias voltage is greater than the AT induced by the temperature gradient, and the net current exhibits conventional transport. However, when $\Delta T > \Delta T_{th}$, the AT induced by the temperature gradient will exceed the forward current, so the net current appears as the ANM, and the ANM gradually increases with the increase of the temperature gradient.

In Fig. 5(b), when the temperature gradient $k_B\Delta T/\hbar\gamma = 5$, it can be found that when a forward bias voltage is applied to the system, the system immediately exhibits the ANM. However, when the bias voltage increases, the forward current generated by the bias voltage will gradually offset the AT, and the ANM will disappear when the bias voltage $\Delta V = \Delta V_{th} = -\varepsilon\ \Delta T/T$. When $\Delta V > \Delta V_{th}$, The steady-state current J_L is always greater than zero and increases with increasing bias voltage.

V. REVERSE HEAT TRANSPORT

Next, we turn to the steady-state flow Q_R with the temperature gradient $k_B\Delta T/\hbar\gamma = 5$. It can be seen from Fig. 6 that when $\Delta V = 0$, the system is only driven by temperature gradient, and the steady-state heat flow Q_R is always greater than zero, that is, the system heat flow flows from the high-temperature reservoir to the low-temperature reservoir. However, when the system superimposes a bias voltage ($|e|\Delta V/\hbar\gamma = 2.5$, $|e|\Delta V/\hbar\gamma = 5$) in the same direction as the temperature gradient, in the region $\varepsilon < 0$, the steady-state heat flow $Q_R < 0$ will appear incredibly. This is an anomalous heat transport, that is, the heat flows from a reservoir with low temperature and low chemical potential to a reservoir with high temperature and high chemical potential. This phenomenon in which the direction of heat flow is opposite to the applied forces (temperature gradient and bias voltage) is called reverse heat transport (RHT). The RHT has been discovered and experimentally verified in thermoelectric materials [33]. In this paper, it is further demonstrated that the RHT effect is also present in quantum dot system, and exhibit other anomalous transport behaviors such as AT and ANM.

Figure 7 shows the curves of the RHT with the bias voltage (a) and the temperature gradient (b), respectively. It can be seen from Fig. 7(a) that when $k_B\Delta T/\hbar\gamma = 5$, the RET occurs in a limited range of the bias voltage, and the RHT first increases and then decreases with the increase of the bias voltage. Figure 7(b) shows that the RHT is induced by the positive bias voltage. When a positive temperature gradient is superimposed on the system, the RHT will be suppressed and eventually the RHT will be transferred to the positive transport with the increase of the temperature gradient.

Figure 8 shows the transport characteristics of the steady-state heat flow Q_L, Q_R, the steady-state current J_L, and the steady-state entropy production rate s of the system when $k_B\Delta T/\hbar\gamma = 5$ and $|e|\Delta V/\hbar\gamma = 5$. It can be found that the system has four transport regions with different characteristics, which are labeled with different background colors. In region 1, the steady-state heat flows Q_L and Q_R of system are positive, while the steady-state current J_L of system is negative. This region exhibits ANM effect. In region 2, $J_L > 0$,

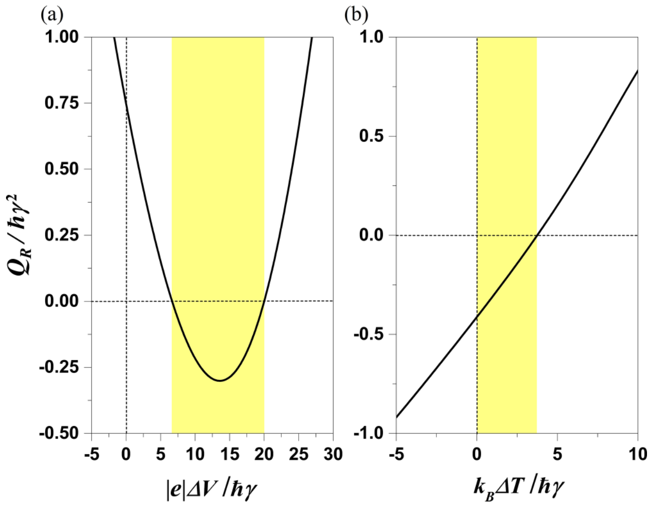

FIG. 7. The steady-state heat flow Q_R is depicted as a function of the bias voltage ΔV for $k_B\Delta T/\hbar\gamma = 5$ (a) and as a function of the temperature gradient ΔT for $|e|\Delta V/\hbar\gamma = 5$ (b), respectively. The reverse heat transport occurs in yellow region. The parameters $k_BT/\hbar\gamma = 7.5$, $\varepsilon/\hbar\gamma = -10$.

while $Q_L < 0$ and $Q_R < 0$. This means that the heat flow in the region flows against the bias voltage and the temperature gradient, that is, the RHT effect. In region 3, $J_L > 0$, $Q_R > 0$, and $Q_L < 0$. In this region, driven by the bias voltage, work (input power $P = J_L\Delta V$) is converted to heat and transferred to two heat reservoirs. The conventional transport processes are located in region 4. In addition, the entropy production rate s is always greater than zero throughout the region. This means that these counterintuitive phenomena do not violate the second law of thermodynamics. In particular, there is a reversible energy level ε_r where $s = 0$. Based on Eq. (9), ε_r is

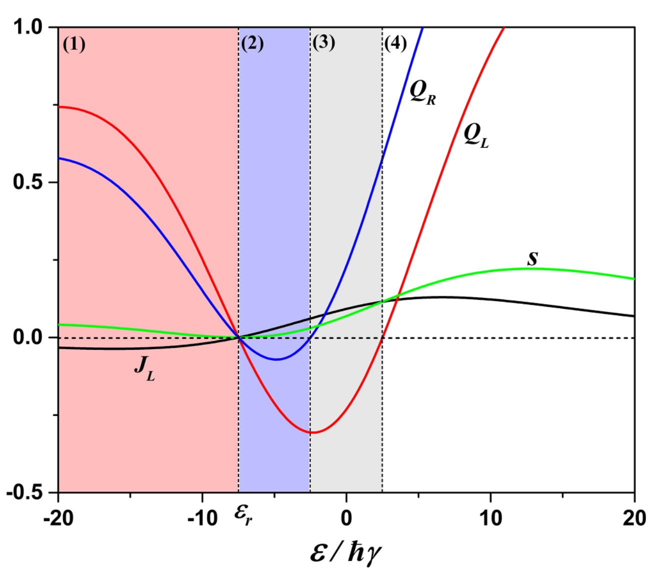

FIG. 8. Anomalous transport. The steady-state heat flow Q_L, Q_R, the steady-state current J_L, and the entropy production rate s are depicted as a function of a single energy level. The parameters $k_BT/\hbar\gamma = 7.5$, $k_B\Delta T/\hbar\gamma = 5$, $|e|\Delta V/\hbar\gamma = 5$.

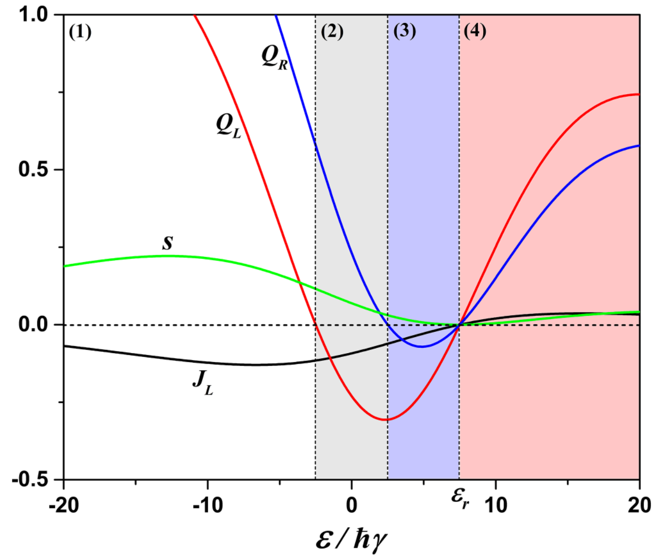

FIG. 9. Thermoelectric transport. The steady-state heat flow Q_L, Q_R, the steady-state current J_L, and the entropy production rate s are depicted as a function of a single energy level. The parameters $k_B\Delta T/\hbar\gamma = 5$, $|e|\Delta V/\hbar\gamma = -5$.

given by

$$\varepsilon_r = \frac{\mu_R T_L - \mu_L T_R}{T_L - T_R}, \tag{10}$$

This reversible energy level distinguishes between the ANM and the RHT. When $\varepsilon < \varepsilon_r$, the system shows the ANM, and when $\varepsilon_r < \varepsilon < \mu_R$, the system shows the RHT.

VI. DISCUSSIONS

For comparison, Fig. 9 shows the steady-state transport characteristics for $k_B\Delta T/\hbar\gamma = 5$, $|e|\Delta V/\hbar\gamma = -5$. In this case, the transport of the system also exists in four different regions. In region 1, the steady-state heat flow and the steady-state current are transported in forward driven by temperature gradient and bias voltage, respectively. In region 2, work is converted to heat and transferred to two heat reservoirs. In region 3, driven by the bias voltage, the steady-state heat flows from the low temperature heat reservoir to the high temperature heat reservoir, then the system is a thermoelectric refrigerator. In region 4, part of the heat output from the high-temperature heat reservoir is used to drive the current to overcome the bias voltage and do work, and the remaining heat is transported to the low-temperature heat reservoir, which is a thermoelectric heat engine. There is a reversible energy level ε_r between the thermoelectric heat engine and the refrigerator, which has the same form as Eq. (10). This is a typical thermoelectric transport phenomenon and has been extensively studied [8–12]. Comparison of o Figs. 8 and 9 reveals that the ANM and the RHT are generated when the external drive is in the same direction, which can be regarded as an equivalent to the thermoelectric transport. The studies presented in this paper offer a new perspective for understanding the thermodynamic properties of steady-state transport of single quantum dot systems.

VII. CONCLUSIONS

We have demonstrated that a single-level quantum dot system deviates from the equilibrium when driven by the temperature gradient and the bias voltage and exhibits three counterintuitive transport phenomena, which are AT, ANM and RHT, respectively. These counterintuitive transport phenomena are attributed to the unbalanced concentration distribution of heat reservoirs on both sides of the energy level. The ANM is essentially a manifestation of the AT when an appropriate bias voltage is applied to the system. The ANM and the RHT can be regarded as equivalent to the thermoelectric transport when the driving force is in the same direction, and there is a reversible energy level that distinguishes between the ANM and the RHT. Although the RHT has been discovered in quantum dot systems [34,35], it is surprising that three counterintuitive transport phenomena can be presented in quantum dot systems, which are interrelated and can be equivalent to thermoelectric transport processes. The results of this paper provide another perspective for understanding the thermodynamic properties of steady-state transport of quantum systems.

ACKNOWLEDGMENTS

Y. Z. acknowledges support by the National Natural Science Foundation of China (Grant No. 12365006) and the Natural Science Foundation of Guangxi (China) (Grant No. 2022GXNSFBA035636). X. Lü acknowledges support by the National Natural Science Foundation of China (Grant No. 12304058) and the Natural Science Foundation of Guangxi (China) (Grant No. 2024GXNSFBA010229).

[1] S. Duhr and D. Braun, Proc. Natl. Acad. Sci. USA. **103**, 19678 (2006).
[2] M. Reichl, M. Herzog, A. Götz, and D. Braun, Phys. Rev. Lett. **112**, 198101 (2014).
[3] A. Barreiro, R. Rurali, E. R. Hernández, J. Moser, T. Pichler, L. Forro, and A. Bachtold, Science **320**, 775 (2008).
[4] H.-R. Jiang, H. Wada, N. Yoshinaga, and M. Sano, Phys. Rev. Lett. **102**, 208301 (2009).
[5] R. de Miguel and J. Miguel Rubí, Phys. Rev. Lett. **123**, 200602 (2019).
[6] D. Pan, H. Xu, and F. Javier García de Abajo, Phys. Rev. Lett. **125**, 176802 (2020).
[7] Y. Zhong and W. Zhong, Physica A **633**, 129406 (2024).
[8] G. Benenti, G. Casati, K. Saito, and R. S. Whitney, Phys. Rep. **694**, 1 (2017).
[9] M. Esposito, K. Lindenberg, and C. Van den Broeck, Europhys. Lett. **85**, 60010 (2009).
[10] M. Josefsson, A. Svilans, A. M. Burke, E. A. Hoffmann, S. Fahlvik, C. Thelander, M. Leijnse, and H. Linke, Nat. Nanotechnol. **13**, 920 (2018).
[11] H. L. Edwards, Q. Niu, and A. L. de Lozanne, Appl. Phys. Lett. **63**, 1815 (1993).
[12] Z. Lin, Y. Yang, W. Li, J. Wang, and J. He, Phys. Rev. E **101**, 022117 (2020).
[13] R. Eichhorn, P. Reimann, and P. Hänggi, Phys. Rev. Lett. **88**, 190601 (2002).
[14] B. Cleuren and C. Van den Broeck, Phys. Rev. E **67**, 055101(R) (2003).
[15] L. Machura, M. Kostur, P. Talkner, J. Łuczka, and P. Hänggi, Phys. Rev. Lett. **98**, 040601 (2007).
[16] J. Luo, K. A. Muratore, E. A. Arriaga, and A. Ros, Anal. Chem. **88**, 5920 (2016).
[17] A. Słapik, J. Łuczka, P. Hänggi, and J. Spiechowicz, Phys. Rev. Lett. **122**, 070602 (2019).
[18] A. Słapik, J. Łuczka, and J. Spiechowicz, Phys. Rev. Appl. **12**, 054002 (2019).
[19] M. Sonker, D. Kim, A. Egatz-Gomez, and A. Ros, Annu. Rev. Anal. Chem. **12**, 475 (2019).
[20] J. Spiechowicz, P. Hänggi, and J. Łuczka, New J. Phys. **21**, 083029 (2019).
[21] M. Wiśniewski and J. Spiechowicz, New J. Phys. **24**, 063028 (2022).
[22] M. Wiśniewski and J. Spiechowicz, Chaos **34**, 073101 (2024).
[23] A. Ros, R. Eichhorn, J. Regtmeier, T. T. Duong, P. Reimann, and D. Anselmetti, Nature (London) **436**, 928 (2005).
[24] J. Nagel, D. Speer, T. Gaber, A. Sterck, R. Eichhorn, P. Reimann, K. Ilin, M. Siegel, D. Koelle, and R. Kleiner, Phys. Rev. Lett. **100**, 217001 (2008).
[25] A. Sarracino, F. Cecconi, A. Puglisi, and A. Vulpiani, Phys. Rev. Lett. **117**, 174501 (2016).
[26] J. Wang, G. Casati, and G. Benenti, Phys. Rev. Lett. **124**, 110607 (2020).
[27] Y. Zhang and Z. Xie, Phys. Rev. E **104**, 064142 (2021).
[28] J. C. Wu, F. J. Lin, and B. Q. Ai, Soft Matter **18**, 1194 (2022).
[29] J. Cividini, D. Mukamel, and H. A. Posch, J. Phys. A Math. Theor. **51**, 085001 (2018).
[30] P. Rizkallah, A. Sarracino, O. Bénichou, and P. Illien, Phys. Rev. Lett. **130**, 218201 (2023).
[31] K. Micadei, J. P. S. Peterson, A. M. Souza, R. S. Sarthour, I. S. Oliveira, G. T. Landi, T. B. Batalhão, R. M. Serra, and E. Lutz, Nat. Comm. **10**, 2456 (2019).
[32] C. L. Latune, I. Sinayskiy, and F. Petruccione, Phys. Rev. Res. **1**, 033097 (2019).
[33] K. Okawa, Y. Amagai, H. Fujiki, and N. H. Kaneko, Comm. Phys. **4**, 267 (2021).
[34] F. Chi, J. Zheng, Y. S. Liu, and Y. Guo, Appl. Phys. Lett. **100**, 233106 (2012).
[35] J. Du, T. Fu, Chen J, S. Su, and J. Chen, Physica A **615**, 128560 (2023).